

Modal strength reduction factors for seismic design of plane steel frames

George A. Papagiannopoulos¹ and Dimitri E. Beskos^{1,2*}

¹*Department of Civil Engineering, University of Patras, 26500 Rio-Patras, Greece*

²*Office of Theoretical and Applied Mechanics, Academy of Athens, 4 Soranou Efessiou str.
11527 Athens, Greece*

(Received September 15, 2010, Accepted November 15, 2010)

Abstract. A new method for the seismic design of plane steel moment resisting frames is developed. This method determines the design base shear of a plane steel frame through modal synthesis and spectrum analysis utilizing different values of the strength reduction (behavior) factor for the modes considered instead of a single common value of that factor for all these modes as it is the case with current seismic codes. The values of these modal strength reduction factors are derived with the aid of a) design equations that provide equivalent linear modal damping ratios for steel moment resisting frames as functions of period, allowable interstorey drift and damage levels and b) the damping reduction factor that modifies elastic acceleration spectra for high levels of damping. Thus, a new performance-based design method is established. The direct dependence of the modal strength reduction factor on desired interstorey drift and damage levels permits the control of deformations without their determination and secures that deformations will not exceed these levels. By means of certain seismic design examples presented herein, it is demonstrated that the use of different values for the strength reduction factor per mode instead of a single common value for all modes, leads to more accurate results in a more rational way than the code-based ones.

Keywords: modal strength reduction (behavior) factor; equivalent linear modal damping ratios; damping reduction factors; interstorey drift; damage; seismic design; steel moment resisting frames.

1. Introduction

According to current codes for the seismic design of structures, the design base shear is calculated by dividing the base shear obtained through modal synthesis in conjunction with an elastic design spectrum by the strength reduction (behavior) factor (e.g. EC8 2004). This factor is also used for the calculation of the deformations of the structure with the aid of the approximate equal-displacement rule. Depending on the type of the structure considered, allowable values for this strength reduction factor are provided in seismic codes (e.g. EC8 2004). However, this constant and common for all modes value of the strength reduction factor does not take into account the particular dynamic characteristics of the structure.

The concept of the strength reduction factor has been the object of extensive research studies

* Corresponding author, Professor, E-mail: d.e.beskos@upatras.gr

since the early works of Veletsos and co-workers (e.g. Veletsos and Vann 1971). Since then, numerous attempts have been made to provide improved expressions for the strength reduction factor in order to better approximate the inelastic behavior of structures (e.g. Miranda and Bertero 1994, Vidic *et al.* 1994, Mazzolani and Piluso 1996, Ordaz and Pérez-Rocha 1998, Borzi and Elnashai 2000, Cuesta *et al.* 2003, Mavroeidis *et al.* 2004, Chakraborti and Gupta 2005, Jalali and Trifunac 2008). Strength reduction factors for single degree-of-freedom (SDOF) systems derived in the aforementioned studies take into account one or more parameters such as, number of earthquake accelerograms, duration of earthquake, rupture distance, earthquake magnitude, near-fault effects, postyield stiffness and hysteresis type, but eventually are expressed in terms of the ductility ratio and the structural period. However, these strength reduction factors do not account for cumulative damage effects as they are based on the assumption that structural damage occurs only due to maximum deformation. Inclusion of cumulative damage effects in strength reduction factors by considering plastic work dissipation in conjunction with earthquake duration and number of inelastic load cycles has been achieved in Mazzolani and Piluso (1996), Chai *et al.* (1998), Kunnath and Chai (2004), Lu and Wei (2008).

Few studies have been performed for obtaining strength reduction factors for multi degree-of-freedom (MDOF) systems. The most common technique is to correlate the required yield strength of a MDOF system with the corresponding one of a SDOF system (Nassar and Krawinkler 1991, Seneviratna and Krawinkler 1997). A different approach is to evaluate strength reduction factors directly on MDOF structural systems using maximum deformation and damage indices (Mwafy and Elnashai 2002, Karavasilis *et al.* 2007).

In spite of all the aforementioned studies, current seismic design codes still use a single common value for all modes for the strength reduction factor mainly derived on the basis of intuition and experience or even on approximate seismic response methods (Englekirk 2008). The need for using different values of the strength reduction factor for different modes computed in a more rational and accurate way has been stressed by Sullivan *et al.* (2008). Towards this direction, the authors have recently developed the equivalent modal damping ratios which, as it has been proved in Papagiannopoulos (2008) and Papagiannopoulos and Beskos (2010), i) can essentially play the role of the strength reduction factor, ii) are given for the first few modes of vibration of the structure that significantly contribute to its dynamic response and iii) can be defined as functions of deformation and damage indices, i.e. interstorey drift and plastic hinge rotation. However, design engineers are more familiar with the concept of the strength reduction factor rather than that of damping. Thus, it is desirable to develop a method of design that employs modal strength reduction factors rather than modal damping.

In this work, on the basis of the equivalent modal damping ratios concept (Papagiannopoulos 2008, Papagiannopoulos and Beskos 2010), it is shown that one can define and compute strength reduction factors with different values for the various modes of the structure. The values of these so-called modal strength reduction factors depend on the type of structure, the type of seismic motion and the desirable level of seismic performance of the structure in terms of acceptable seismic deformation and damage. Therefore, a departure from the usual consideration of the common single value of the strength reduction factor for all modes in seismic codes is proposed. Since the proposed modal strength reduction factor has different values for each mode, the estimation of seismic displacements of the structure via the equal-displacement approximation does not hold. However, this is not a matter of concern because the value of the modal strength reduction factor is given herein as a function of bounded seismic performance levels in terms of both

deformation (interstorey drift) and damage (plastic hinge rotation). Thus, seismic displacements, although not calculated, cannot exceed these acceptable seismic performance levels. At this point, one could mention the work of Takewaki (1997) dealing with bounds on deformation (ductility) of plane frames under seismic loading.

The deformation and damage dependent modal strength reduction factor is found by performing a per mode inversion of the damping reduction factor used to construct an elastic acceleration spectrum for an amount of damping ratio higher than the typically considered 5% value. This damping reduction factor is calculated per mode on the basis of deformation and damage dependent equivalent modal damping ratios developed in Papagiannopoulos (2008) and Papagiannopoulos and Beskos (2010) with the aid of extensive parametric studies. However, it should be noted that the aforementioned highly damped spectra correspond to absolute acceleration and not to pseudo-acceleration for reasons explained in Papagiannopoulos (2008) and Papagiannopoulos and Beskos (2010). Therefore, a) a comparison between the modal strength reduction factors associated with pseudo-acceleration and absolute acceleration spectra is used and b) a period and damping dependent conversion factor is proposed to be used in conjunction with the 5% damped pseudo-acceleration spectral values in order to transform these values into absolute acceleration ones (Weitzmann *et al.* 2006).

The modal strength reduction factor is finally employed to perform the seismic design of plane moment resisting steel frames. The design seismic base shear of the frame is determined by modal synthesis and spectrum analysis on the basis of different values of the strength reduction factor for the first few modes. This design base shear is first compared with the one coming from non-linear dynamic analysis. A second comparison is then performed against the usual procedure of seismic codes that makes use of a single common value of the strength reduction factor for all modes and of pseudo-acceleration spectra.

On the basis of the examples presented, it is concluded that the use of the modal strength reduction factor instead of the single value one, leads to more accurate design base shear results in a more rational way. Moreover, the direct dependence of the modal strength reduction factor on deformation and damage makes any displacement evaluation unnecessary and thus the use of the equal-displacement approximation is avoided.

2. Review on equivalent modal damping ratios

2.1 The equivalent modal damping ratios concept

According to the developments in Papagiannopoulos (2008) and Papagiannopoulos and Beskos (2010), a non – linear MDOF structure can be substituted for seismic response purposes by an equivalent linear MDOF structure having the same mass and initial stiffness with the non – linear one and linear equivalent modal damping ratios that take into account the effects of all non – linearities, which, however, should not be highly localized. The conversion of the effects of non – linearities into equivalent modal damping ratios is based on a balance (equivalence) between the work due to linear damping and that due to non – linearities. This equivalence is accomplished with the aid of a modal damping identification model based on the modulus of the roof-to-basement frequency response transfer function $R(\omega)$ evaluated at the resonant frequency ω_k of a linear plane framed structure, which reads as (Papagiannopoulos 2008, Papagiannopoulos and Beskos 2010)

$$\begin{aligned}
|R(\omega = \omega_k)|^2 = & 1 + 2 \sum_{j=1}^N \frac{\phi_{rj} \Gamma_j \omega_k^2 (\omega_j^2 - \omega_k^2)}{(\omega_j^2 - \omega_k^2)^2 + (2\xi_j \omega_j \omega_k)^2} + \sum_{j=1}^N \frac{[\phi_{rj}^2 \Gamma_j^2 \omega_k^4 (\omega_j^2 - \omega_k^2) + 4\xi_j^2 \omega_j^2 \omega_k^2]}{[(\omega_j^2 - \omega_k^2)^2 + (2\xi_j \omega_j \omega_k)^2]^2} + \\
& + 2 \sum_{j \neq m, m > j}^N \frac{\phi_{rj} \Gamma_j \phi_{rm} \Gamma_m \omega_k^4 [(\omega_j^2 - \omega_k^2)(\omega_m^2 - \omega_k^2) + 4\xi_j \xi_m \omega_j \omega_m \omega_k^2]}{[(\omega_j^2 - \omega_k^2)^2 + (2\xi_j \omega_j \omega_k)^2][(\omega_m^2 - \omega_k^2)^2 + (2\xi_m \omega_m \omega_k)^2]}
\end{aligned} \quad (1)$$

Eq. (1) represents a system of N nonlinear algebraic equations which, on the assumption that $|R(\omega = \omega_k)|$, the undamped modal shapes ϕ_{rj} , the resonant frequencies ω_k and the corresponding participation factors Γ_j are known, can be solved numerically to obtain the modal damping values ξ_k . Modal damping values can be found only for the modes that appear in the transfer function.

When the framed structure under study is linear, the modulus of the transfer function $|R(\omega)|$ has a smooth shape with well defined visible peaks (resonant frequencies) and the solution of Eq. (1) is straightforward. When the structure is non – linear, the transfer function does not have a smooth shape. In this case, one may iteratively transform this transfer function into a smooth one by ‘feeding’ the structure with continuously increasing amounts of damping till $|R(\omega)|$ and $|dR(\omega)/d(\omega)| = |R'(\omega)|$ achieve a smooth shape, indicating that all non – linearities have vanished and the structure has become an equivalent linear one. Figs. 1 and 2 show the curves of the modulus of the transfer function versus frequency for an original SDOF non-linear structure and its equivalent linear one, respectively. For the equivalent linear structure, Eq. (1) can be solved and provide the equivalent modal damping ratios. To ensure the smooth shape of $|R(\omega)|$ and $|R'(\omega)|$, certain smoothness criteria have to be satisfied as explained in detail in Papagiannopoulos (2008) and Papagiannopoulos and Beskos (2010).

The equivalent modal damping ratios can be viewed as playing the role of the strength reduction factor in seismic design in a more rational and accurate way. They can also be given as functions of deformation and damage and, thus, can be directly implemented to the seismic design of a structure (Papagiannopoulos 2008, Papagiannopoulos and Beskos 2010). Design equations providing equivalent damping ratios as functions of period and allowable deformation and damage for the first few significant modes have been constructed using extensive numerical data coming from a

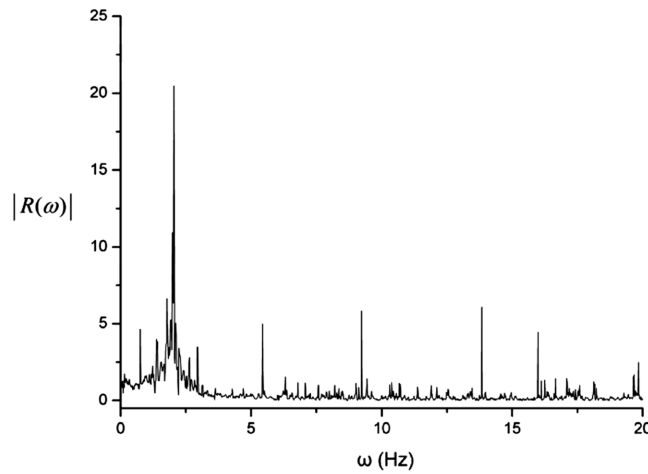


Fig. 1 $|R(\omega)|$ for a non-linear SDOF structure

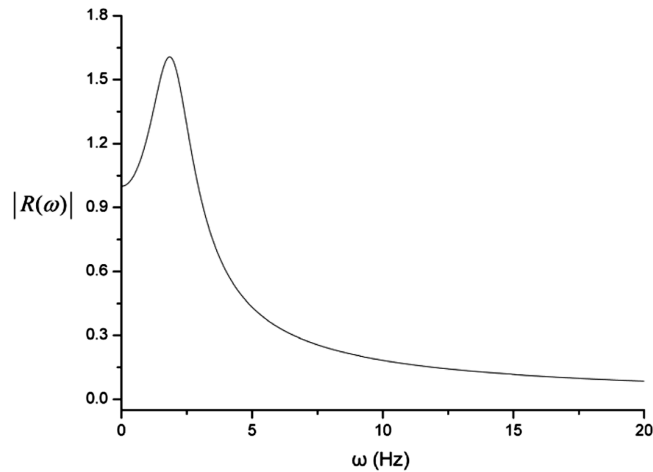


Fig. 2 $|R(\omega)|$ for an equivalent linear SDOF structure

representative number of plane steel moment resisting frames excited by various seismic motions (Papagiannopoulos 2008, Papagiannopoulos and Beskos 2010). These design equations are used in conjunction with an elastic spectrum, constructed so as to accommodate high damping values, and modal synthesis tools to calculate the design forces of the structure. The numerical data and the computational procedure used to construct the design equations providing equivalent damping ratios as functions of period and allowable deformation and damage for the first few significant modes as well as the highly damped elastic spectra are summarized in the following subsection.

2.2 Steel frames, earthquake ground motions and seismic performance levels

A set of 20 steel plane moment resisting frames was used for the parametric analyses. The frames are regular and orthogonal with storey heights and bay widths equal to 3.0 m and 4.0 m respectively. The number of stories and bays varies taking the values of 2, 3, 4, 7, 9, 12, 15, 18 and 1, 2, 3, 4, 5, 6, respectively. The frames have been designed in accordance with the provisions of EC 3 (1992) and EC 8 (2004) assuming an acceleration design spectrum with a peak ground acceleration (PGA) equal to 0.24 g, a soil of class B and a strength reduction (behavior) factor equal to 3. Load on beams (dead and live loads of the floors) is constant for each frame and takes values between 25 and 30 kN/m in order to ensure different fundamental periods for the frames examined. The yield stress of the steel material was set equal to 275 MPa.

The analytical models of the frames were centreline representations with two finite elements per physical member of the frame. Material inelastic behavior was modelled by means of bilinear point plastic hinges with 3% hardening. The frame connections were assumed to be rigid without incorporation of the strength and stiffness of the panel zones. Diaphragm action was assumed at every floor due to the presence of the slab. Data for the steel frames, including number of bays, number of stories, European beam (IPE) and column (HEB) sections and first and second natural periods of vibration are shown in Table 1 (Papagiannopoulos and Beskos 2010). In this Table, expressions of the form, e.g. 400/450/450/450/400-400 (1-5) mean that a) from the first to the fifth storey the columns and beams have the same variation at every storey and b) at every storey one has column sections HEB 400 and HEB 450 for the first bay, HEB 450 and HEB 450 for the next

Table 1 Steel moment resisting frames considered

Frame	Number of stories	Number of bays	Sections Columns: (HEB) & Beams: (IPE)	Period T ₁ (sec)	Period T ₂ (sec)
1	2	1	220-270 (1-2)	0.51	0.15
2	3	1	240-270 (1-3)	0.62	0.18
3	4	2	260-330 (1-4)	0.69	0.21
4	4	2	240-330 (1-4)	0.76	0.24
5	4	2	240-330 (1-4)	0.83	0.26
6	7	2	300-400 (1-7)	0.96	0.31
7	7	2	300-360 (1-4) & 280-360 (5-7)	1.07	0.35
8	7	2	330-330 (1-4) & 260-330 (5-7)	1.29	0.42
9	9	3	360/400/400/360-400 (1-4) & 340/360/360/340-400 (5-9)	1.13	0.37
10	9	3	360/400/400/360-400 (1-4) & 340/360/360/340-400 (5-9)	1.24	0.40
11	9	3	360/400/400/360-400 (1-4) & 320/360/360/320-400 (5-9)	1.38	0.45
12	12	4	340/360/400/360/340-450 (1-4) & 320/340/360/340/ 320-450 (5-8) & 300/320/340/320/300-450 (9-12)	1.43	0.48
13	12	4	340/360/400/360/340-400 (1-4) & 320/340/360/340/320-400 (5-8) & 300/320/340/320/300-400 (9-12)	1.58	0.52
14	12	4	340/360/400/360/340-400 (1-4) & 320/340/360/340/320-400 (5-6) & 320/340/360/340/320-360 (7-8) & 300/320/340/320/300-360 (9-12)	1.65	0.57
15	15	5	450/450/500/500/450/450-450 (1-4) & 400/450/450/450/450/400-450 (5-8) & 360/400/450/450/400/360-450 (9-12) & 340/360/400/400/360/340-450 (13-15)	1.76	0.58
16	15	5	400/450/500/500/450/400-450 (1-4) & 400/400/450/450/400/400-450 (5-8) & 360/400/400/400/400/360-450 (9) & 360/400/400/400/400/360-400 (10-12) & 340/360/400/400/360/340-400 (13-15)	1.88	0.64
17	15	5	450/450/500/500/450/450-400 (1-4) & 400/450/450/450/450/400-400 (5-8) & 360/400/450/450/400/360-400 (9) & 340/360/400/400/360/340-360 (10-12) & 340/360/400/400/360/340-360 (13-15)	2.02	0.69
18	18	6	550/550/600/600/600/550/550-400 (1-6) & 500/500/550/550/550/500/500-400 (7-12) & 450/450/500/500/500/450/450-360 (13-18)	2.18	0.75
19	18	6	550/550/600/600/600/550/550-400 (1-6) & 500/500/ 550/550/550/500/500-400 (7-10) & 500/500/550/550/550/500/500-360 (11-12) & 450/450/500/500/500/450/450-360 (13-18)	2.30	0.80
20	18	6	550-400 (1-6) & 500-400 (7-12) & 450-360 (13-18)	2.42	0.85

Table 2 List of earthquake ground motion records considered

Earthquake, Location	Date	Station	M_w	Fault Mechanism ^a	Site code ^b	Recorded PGA (m/sec ²)	Recorded PGV (m/sec)	Type of motion
Tokachi Oki, Japan	16/05/1968	HAC1*	7.90	RV	SL	2.06	0.39	Long duration
		HAC2*			SL	3.18	0.43	Long duration
San Fernando, U.S.A.	09/02/1971	PCD	6.60	RV	HR	12.03	1.12	Pulse
Gazli, Former U.S.S.R.	17/05/1976	KAR	6.80	RV	SR	6.04	0.51	Pulse
Bucharest, Romania	04/03/1977	BRI	7.40	RV	SL	1.98	0.73	Pulse
Tabas, Iran	16/09/1978	TAB	7.10	RV	SL	9.09	0.85	Pulse
Imperial Valley, U.S.A.	15/10/1979	E05	6.50	SS	SL	3.72	0.91	Pulse
		E06			SL	4.31	1.10	Pulse
		E07			SL	4.55	1.09	Pulse
Valparaiso, Chile	03/03/1985	LLO	7.90	RV	SR	6.63	0.39	Long duration
		LLA			SL	4.56	0.37	Long duration
		VDM			SR	3.56	0.33	Long duration
		ISI			?	6.68	0.41	Long duration
Michoachan, Mexico	19/09/1985	SCT	8.00	RV	SL	1.62	0.72	Long duration
Superstition Hills, U.S.A.	24/11/1987	PTS	6.50	SS	?	4.47	1.12	Pulse
Loma Prieta, U.S.A.	17/10/1989	LGP	7.00	OB	HR	5.53	0.95	Pulse
		COR			SR	5.94	0.51	Pulse
Manjil, Iran	20/06/1990	AT2	7.40	SS	?	4.87	0.52	Long duration
Erzincan, Turkey	13/03/1992	ERZ	6.70	SS	SL	5.05	0.84	Pulse
Petrolia, U.S.A.	25/04/1992	CAP	6.90	RV	HR	14.69	2.50	Pulse
Landers, U.S.A.	28/06/1992	LUC	7.30	SS	SL	7.17	1.86	Pulse
Northridge, U.S.A.	17/01/1994	RRS	6.70	RV	SL	8.22	1.66	Pulse
		NWH1*			SL	5.72	0.75	Pulse
		NWH2*			SL	5.79	0.97	Pulse
		SCG1*			SL	6.00	1.17	Pulse
		SCG2*			SL	8.80	1.02	Pulse
Kobe, Japan	17/01/1995	TAK	6.90	SS	SL	6.00	1.28	Pulse
Izmit, Turkey	17/08/1999	SKR	7.40	SS	SR	3.69	0.79	Pulse
Chi-Chi, Taiwan	20/09/1999	TCU 052	7.60	OB	SL	3.42	1.80	Pulse
		TCU 068			SL	4.93	2.75	Pulse
Duzce, Turkey	12/11/1999	BOL	7.10	SS	SL	7.31	0.54	Pulse
El Salvador, El Salvador	13/01/2001	OB	7.60	NM	SR	4.00	0.36	Long duration
		ST			SR	7.28	0.41	Long duration
Tokachi Oki, Japan	25/09/2003	HKD 092	8.00	RV	SL	5.70	0.54	Long duration
		HKD 100			?	9.23	0.53	Long duration
Ica Pisca, Peru	15/08/2007	ICA2	8.00	?	?	3.35	0.64	Long duration

^aHorizontal components of the same recording; ^aSS: Strike-Slip; RV: Reverse; OB: Oblique; NM: Normal; ^bHR: Hard Rock; SR: Sedimentary and Conglomerate Rock; SL: Soil and Alluvium; ?: Unknown.

Table 3 Design equations for equivalent modal damping ξ_k for various values of IDR and θ_p

Seismic motions	Mode	IDR = 0.6%	IDR = 1.5% & $\theta_p = \theta_y$	IDR = 2.0% & $\theta_p = 3.5\theta_y$	IDR = 2.5% & $\theta_p = 6\theta_y$
$M_w \leq 6.8$	1	$\xi = 0.015$ for $0.5 \leq T \leq 2.5$ sec	$\xi = 0.08$ for $0.5 \leq T \leq 2.5$ sec	-	$\xi = 0.26 - 0.19 \cdot (T - 1.5)$ for $0.5 \leq T \leq 1.5$ sec & $\xi = 0.26$ for $1.5 \leq T \leq 2.5$ sec
	2	$\xi = 0.006$ for $0.15 \leq T \leq 0.85$ sec	$\xi = 0.045$ for $0.15 \leq T \leq 0.85$ sec	-	-
	3	$\xi = 0.006$ for $0.11 \leq T \leq 0.48$ sec	$\xi = 0.275 \cdot (T - 0.3) + 0.025$ for $0.3 \leq T \leq 0.5$ sec	-	-
	4	$\xi = 0.006$ for $0.11 \leq T \leq 0.32$ sec	-	-	-
	5	$\xi = 0.005$ for $0.10 \leq T \leq 0.24$ sec	-	-	-
$M_w > 6.8$	1	$\xi = 0.01$ for $0.5 \leq T \leq 2.5$ sec	$\xi = 0.08$ for $0.5 \leq T \leq 2.5$ sec	-	$\xi = 0.38$ for $0.5 \leq T \leq 2.5$ sec
	2	$\xi = 0.04$ for $0.15 \leq T \leq 0.85$ sec	$\xi = 0.06$ for $0.15 \leq T \leq 0.85$ sec	-	$\xi = 0.10$ for $0.15 \leq T \leq 0.85$ sec
	3	$\xi = 0.003$ for $0.11 \leq T \leq 0.48$ sec	$\xi = 0.05$ for $0.3 \leq T \leq 0.35$ sec & $\xi = 0.615 \cdot (T - 0.35) + 0.05$ for $0.35 \leq T \leq 0.48$ sec	-	-
	4	$\xi = 0.006$ for $0.11 \leq T \leq 0.32$ sec	-	-	-
	5	$\xi = 0.007$ for $0.10 \leq T \leq 0.24$ sec	-	-	-
Long duration	1	$\xi = 0.015$ for $0.5 \leq T \leq 2.5$ sec	$\xi = 0.025 \cdot (T - 0.5) + 0.10$ for $0.5 \leq T \leq 2.5$ sec	$\xi = 0.47$ for $0.5 \leq T \leq 2.5$ sec	-
	2	$\xi = 0.005$ for $0.15 \leq T \leq 0.85$ sec	$\xi = 0.055$ for $0.15 \leq T \leq 0.85$ sec	$\xi = 0.11$ for $0.15 \leq T \leq 0.85$ sec	-
	3	$\xi = 0.004$ for $0.11 \leq T \leq 0.48$ sec	$\xi = 0.035$ for $0.11 \leq T \leq 0.48$ sec	$\xi = 0.10$ for $0.32 \leq T \leq 0.47$ sec	-
	4	$\xi = 0.004$ for $0.11 \leq T \leq 0.32$ sec	$\xi = 0.035$ for $0.11 \leq T \leq 0.27$ sec & $\xi = 0.8 \cdot (T - 0.27) + 0.035$ for $0.27 \leq T \leq 0.32$ sec	-	-
	5	$\xi = 0.004$ for $0.10 \leq T \leq 0.24$ sec	$\xi = 0.929 \cdot (T - 0.17) + 0.035$ for $0.17 \leq T \leq 0.24$ sec	-	-

two bays and HEB 450 and HEB 400 for the last bay and that all beams have IPE 400 sections.

A total of 36 historical earthquake accelerograms recorded worldwide from 24 different earthquake events from 1968 to 2007 have been used in this work. The set of accelerograms includes earthquake ground motions recorded in the proximity of faults (near fault pulse type ground motions) and earthquake ground motions exhibiting long duration, recorded in areas affected by subduction zones. Table 2 taken from Papagiannopoulos and Beskos (2010) provides information regarding the location, date, magnitude and fault mechanism of every earthquake event as well as the station name, the site code and the recorded peak ground acceleration (PGA) and peak ground velocity (PGV) of the accelerograms considered. Pictorial representations of the acceleration and velocity histories of these seismic motions can be found in Papagiannopoulos (2008).

Interstorey drift ratio (IDR) is used as a measure of the deformation performance of the frames. Regarding the damage performance of the frames, the rotational capacity of the plastic hinge θ_p is used. The maximum acceptable values of IDR and θ_p for the steel frames considered here are shown at the top line of Table 3 taken from Papagiannopoulos and Beskos (2010).

2.3 Absolute acceleration spectra for high damping values

The seismic design method based on equivalent modal damping ratios (Papagiannopoulos 2008, Papagiannopoulos and Beskos 2010) requires the availability of elastic absolute acceleration response/design spectra with amounts of damping much higher than 5% (up to 50% and 100% for overdamped modes). These highly damped spectra correspond to absolute acceleration and not to pseudo-acceleration because the equivalent damping forces, which are characterized by high amounts of damping, actually replace the nonlinear restoring forces and are by no means negligible. Similar considerations can also be found in Lin and Chang (2003) and Weitzmann (2006).

The absolute acceleration response spectrum S_a^r is constructed using the maximum values of the absolute acceleration for a family of SDOF systems having periods from 0.01 to 3 sec in steps of 0.00025 sec, a fixed damping ratio of 5, 10, 15, 20, 25, 30, 40, 50, 60, 75, 100% and subjected to a given seismic motion. Absolute acceleration design spectra S_a are then constructed based on the median and on the median plus one standard deviation response acceleration spectra S_a^r of the 36 seismic motions considered here. For reasons explained in Papagiannopoulos (2008) and Papagiannopoulos and Beskos (2010), pulse type motions have been separated according to the magnitude of the seismic moment M_w of these motions into two categories: those having $M_w \leq 6.8$ (moderate events) and those having $M_w > 6.8$ (moderate-to-large events). Mean and mean plus one deviation design acceleration spectra for pulse motions having $M_w \leq 6.8$, pulse motions having $M_w > 6.8$ and long duration motions have been constructed and can be found in Papagiannopoulos (2008) and Papagiannopoulos and Beskos (2010).

2.4 Design equations for equivalent modal damping ratios

The 20 steel frames were analyzed by the well-known program DRAIN-2DX (Prakash *et al.* 1993) to determine their response to each of the 36 earthquake ground motions considered. The roof-to-basement transfer function was iteratively constructed and checked against the satisfaction of the smoothness criteria mentioned in Papagiannopoulos (2008) and Papagiannopoulos and Beskos (2010). The design equations of equivalent modal damping ratios as function of period and seismic performance limit states are given in Table 3 for three separate cases of ground motions: pulse type

motions having $M_w \leq 6.8$, pulse type motions having $M_w > 6.8$ and long duration motions (Papagiannopoulos and Beskos 2010). In those tables a dash (-) is used for the modes that do not appear in the transfer function and implies that a damping of 100% has to be considered for them.

3. The modal strength reduction factor

Taking into account the developments in Papagiannopoulos (2008) and Papagiannopoulos and Beskos (2010), the equivalent modal damping ratios are considered to be properties of an imaginary equivalent linear MDOF system and are derived by using the response of the original non – linear MDOF system by means of an iterative process. These damping ratios play the role of the strength reduction factor and may correspond to any desired level of deformation and damage. Therefore, they can be viewed as structural properties that are directly related to the modes of the structure. Use of these modal damping ratios in conjunction with an acceleration spectrum and modal synthesis can provide the seismic design force. Computation of displacements is not needed since these are controlled automatically through the deformation and damage dependence of the modal damping ratios and thus the use of the equal displacement approximation is avoided.

However, the concept of the strength reduction factor in seismic design is conceptually simpler and more familiar to engineers as being closer to the existing code-based methods. Therefore, the rest of this section is devoted to the construction of modal strength reduction factors as an alternative to the equivalent modal damping ratios developed previously. This is materialized as follows

Firstly, the damping reduction factor B_a is defined as

$$B_a = |\ddot{u}_l|_{max} / |\ddot{u}_l|_{max, \xi=5\%} = S_a(T, \xi) / S_a(T, 5\%) \quad (2)$$

where \ddot{u}_l is the absolute acceleration, ξ is the damping ratio, $S_a(T, 5\%)$ the absolute acceleration of the structure for 5% damping and $S_a(T, \xi)$ the absolute acceleration of the structure for other than 5% damping. The value of 5% damping corresponds to the damping typically assumed in seismic codes for the linear range of response. Each modal contribution to the seismic design force is given as $M_k^* \cdot S_{a,k}(T_k, \xi_{eq,k})$, where M_k^* is the effective modal mass of mode k and $S_{a,k}(T_k, \xi_{eq,k})$ is the corresponding acceleration spectrum ordinates computed at natural period T_k and equivalent damping $\xi_{eq,k}$. The total seismic design force is derived by combining the individual modal contributions mentioned above by using an appropriate modal combination rule. Thus, one can define the modal strength reduction factor q_k as the ratio of the modal elastic base shear $V_{el,k}$ of a structure over its corresponding modal yielding base shear $V_{y,k}$. More specifically, using the effective modal mass M_k^* as well as $S_{a,k}(T_k, \xi_{el,k})$ and $S_{a,k}(T_k, \xi_{eq,k})$ as the corresponding acceleration spectrum ordinates computed at natural period T_k and damping $\xi_{el,k}$ and $\xi_{eq,k}$ respectively, one has that

$$q_k = V_{el,k} / V_{y,k} = M_k^* S_{a,k}(T_k, \xi_{el,k}) / M_k^* S_{a,k}(T_k, \xi_{eq,k}) = S_{a,k}(T_k, \xi_{el,k}) / S_{a,k}(T_k, \xi_{eq,k}) \quad (3)$$

The modal elastic base shear $V_{el,k}$ is the one computed for the damping value $\xi_{el,k} = 5\%$ used in seismic codes. Using now the definition of the damping reduction factor as given in Eq. (2), one has that

$$q_k = S_{a,k}(T_k, \xi_{el,k}) / S_{a,k}(T_k, \xi_{eq,k}) = 1 / B_{a,k} \tag{4}$$

where $B_{a,k}$ denotes the modal damping reduction factor. Therefore, the values of the modal strength reduction factor can be derived by inverting those of the modal damping reduction factor. In other words, the reduction of the seismic design force, as effected by the strength reduction factor, theoretically coincides with the reduction of the seismic force as affected by the damping reduction factor. Equivalent damping constitutes the connecting link between these two reduction factors.

Adopting the present modal strength reduction factor approach in conjunction with the usual acceleration spectrum for 5% damping, the standard concept of earthquake engineering to reduce seismic elastic forces through the use of a strength reduction factor acquires a solid physical basis because now the structure is treated as a MDOF system for which a different value of the strength reduction factor is assigned to each mode in contrast to the usual consideration in seismic codes where a single common value of the strength reduction factor is assigned to all modes.

4. Curves and design equations for modal strength reduction factors

Mean and mean plus one deviation values of the damping reduction factor B_a have been calculated on the basis of the mean and mean plus one deviation absolute acceleration spectra of the aforementioned three categories of seismic motions. Thus, using Eq. (4), one can obtain the variation of the strength reduction factor with period. Figs. 3 and 4 display the mean and mean plus one deviation values of the strength reduction factor q_k versus period for long duration motions. In these figures the ratio 5% / ξ % symbolizes the ratio $S_a(5\%) / S_a(\xi\%)$. Similar figures can be constructed for the case of pulse type motions having $M_w \leq 6.8$ and $M_w > 6.8$ but are not presented herein due to space limitations.

However, these values of the strength reduction factor q_k correspond to absolute acceleration and cannot be used for spectrum analysis associated with pseudo-acceleration spectra, which is the case

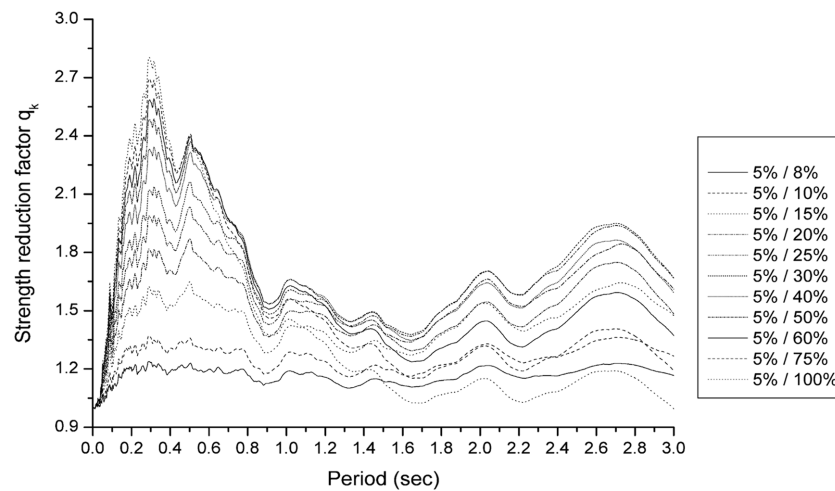


Fig. 3 Mean values of the strength reduction factor versus period from mean absolute acceleration spectra for long duration motions

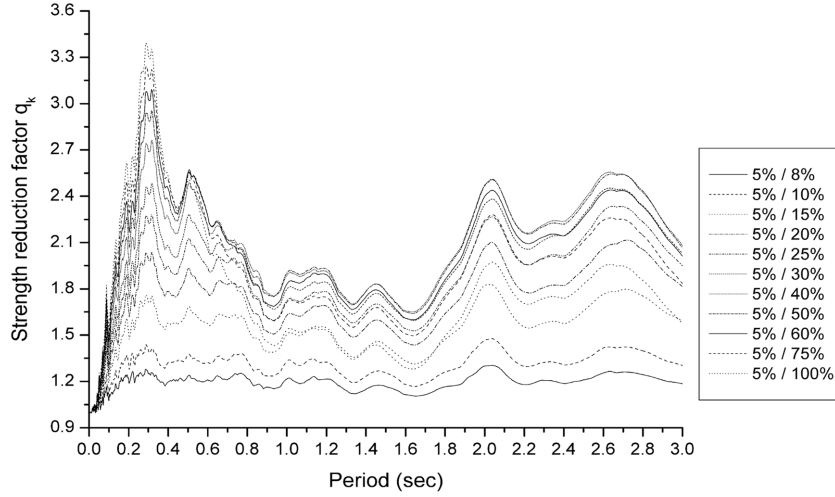


Fig. 4 Mean values plus one deviation values of the strength reduction factor versus period from mean plus one deviation absolute acceleration spectra for long duration motions

in practical seismic design. For this reason one needs to establish a way to go from absolute acceleration spectral values to pseudo-acceleration ones and vice-versa. This can be accomplished as follows:

First the damping reduction factor \bar{B}_a associated with pseudo-acceleration spectra is defined on the basis of Eq. (2) and reads as

$$\bar{B}_a = PS_a(T, \xi) / PS_a(T, 5\%) \quad (5)$$

where $PS_a(T, \xi)$ and $PS_a(T, 5\%)$ are the pseudo-acceleration spectral values for damping ξ and 5%, respectively. This factor is calculated on the basis of the mean and mean plus one deviation pseudo-acceleration spectra of the aforementioned three categories of seismic motion and its mean and mean plus one deviation values are recorded. The procedure of constructing pseudo-acceleration spectra follows the one for absolute acceleration spectra mentioned in section 2.3. Thus, having in mind Eqs. (4) and (5), one can define for mode k the strength reduction factor \bar{q}_k versus period associated with pseudo-acceleration spectra as

$$\bar{q}_k = PS_{a,k}(T_k, \xi_{el,k}) / PS_{a,k}(T_k, \xi_{eq,k}) = 1 / \bar{B}_{a,k} \quad (6)$$

Figs. 5 and 6 show the mean and mean plus one deviation values of the strength reduction factor \bar{q}_k versus period from mean and mean plus one deviation pseudo-acceleration spectra, respectively, for long duration motions. In these figures the ratio 5% / ξ % symbolizes the ratio $PS_a(5\%) / PS_a(\xi\%)$. Similar figures can be constructed for the case of pulse type motions having $M_w \leq 6.8$ and $M_w > 6.8$ but are not presented herein due to space limitations. As one may conclude from Figs. 3-6, the values of \bar{q}_k associated with pseudo-acceleration spectra approach the values found in the literature but are theoretically incorrect in comparison to the values of q_k associated with absolute acceleration spectra. In general, one has $\bar{q}_k > q_k$.

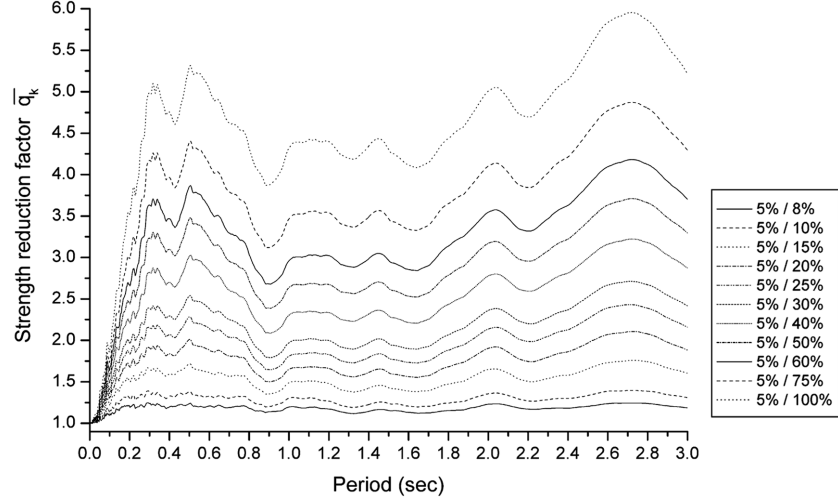


Fig. 5 Mean values of the strength reduction factor versus period from mean pseudo-acceleration spectra for long duration motions

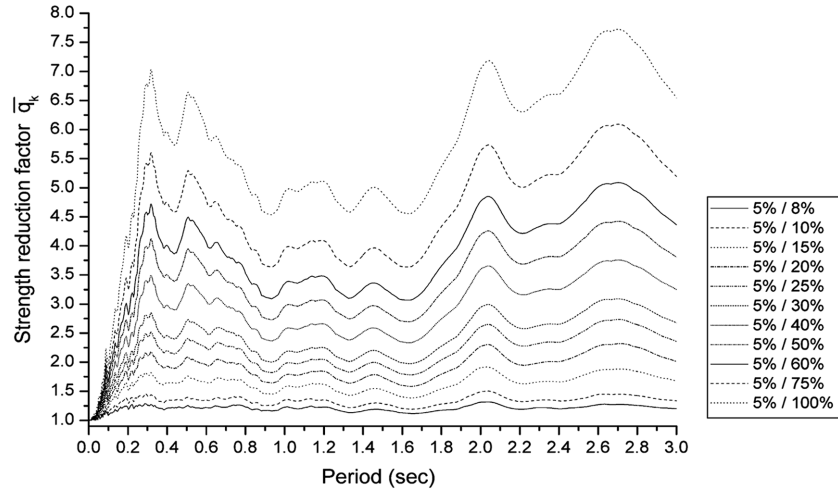


Fig. 6 Mean plus one deviation values of the strength reduction factor versus period from mean plus one deviation pseudo-acceleration spectra for long duration motions

Introduction of the ratio n defined as

$$n = S_a(T, \xi) / PS_a(T, \xi) \quad (7)$$

where $S_a(T, \xi)$ and $PS_a(T, \xi)$ denote the values of absolute acceleration and pseudo-acceleration, respectively, for given values of period T and damping ξ enable one to construct Figs. 7 and 8 which display the mean and mean plus one deviation values of this ratio for long duration motions. Finally, combining Eqs. (5) and (7) one can obtain the desired relation between pseudo-acceleration spectral values for 5% and absolute acceleration spectral values for damping ξ in the form

$$S_a(T, \xi) = \lambda \cdot PS_a(T, 5\%) \quad (8)$$

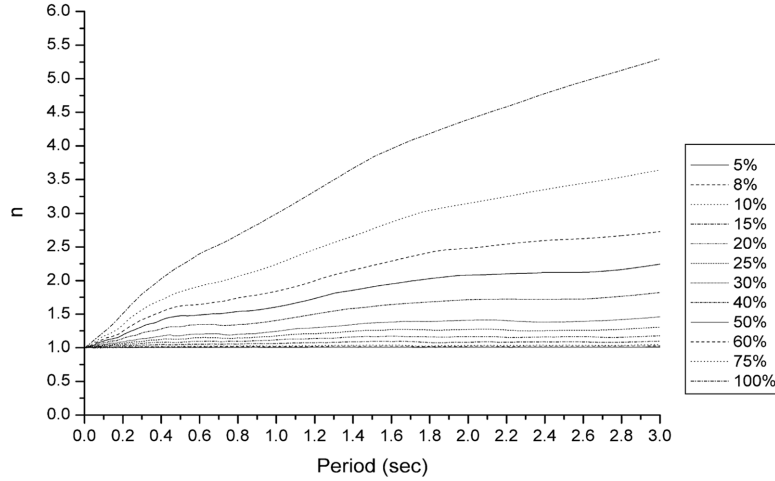


Fig. 7 Mean values of the ratio n versus period for long duration motions

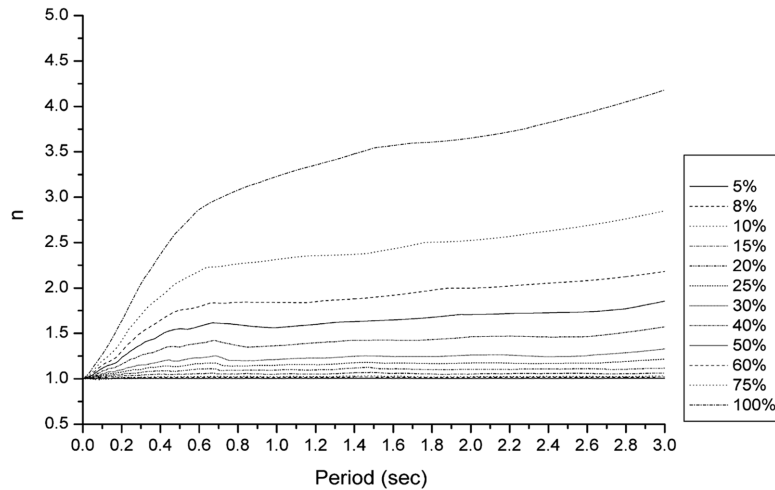


Fig. 8 Mean plus one deviation values of the ratio n versus period for long duration motions

where the conversion factor $\lambda = n \cdot \bar{B}_a$ is a function of period and damping. Figs. 9 and 10 display the mean and mean plus one deviation values of λ as functions of period and damping for long duration motions, while Table 4 provides the corresponding algebraic expressions for this factor λ . It should be noted that since $S_a(T, 5\%) \cong PS_a(T, 5\%)$, one has $\lambda = 1$ when $\xi = 5\%$. Similar figures and equations can be given for the case of pulse type motions having $M_w \leq 6.8$ and $M_w > 6.8$ but are not presented herein due to space limitations.

Figs. 3 and 4 for the modal strength reduction factor q_k cannot be directly used for design purposes because they do not show their deformation and damage dependence. By combining these figures with the deformation and damage dependent equivalent modal damping values of Table 3, one can obtain the mean and mean plus one deviation values of the modal strength reduction factor as functions of period, deformation and damage. To maintain consistency with the damping

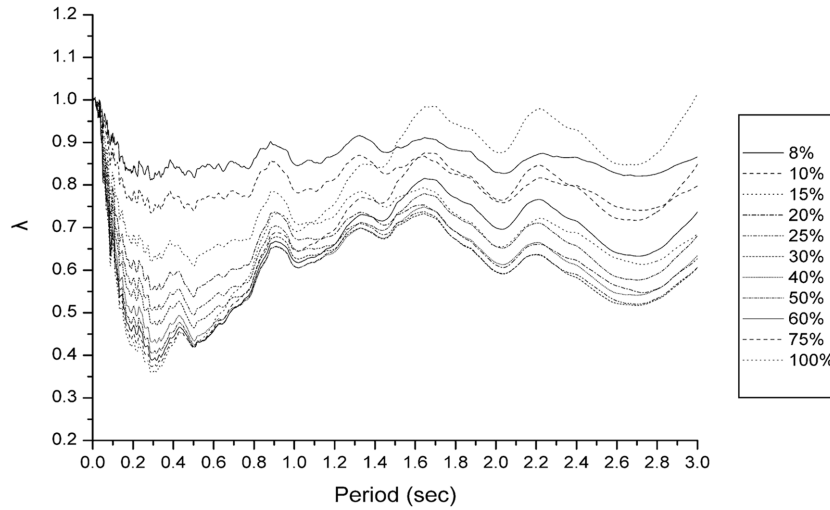


Fig. 9 Mean values of λ versus period for long duration motions

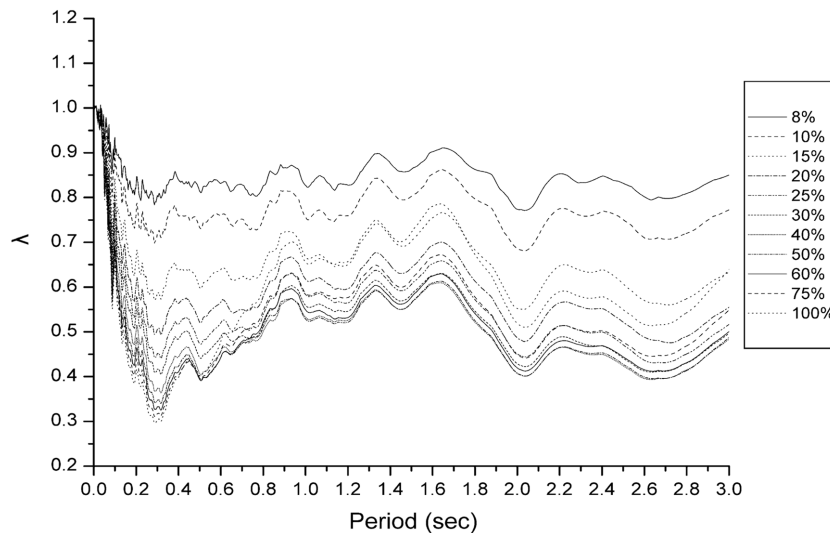


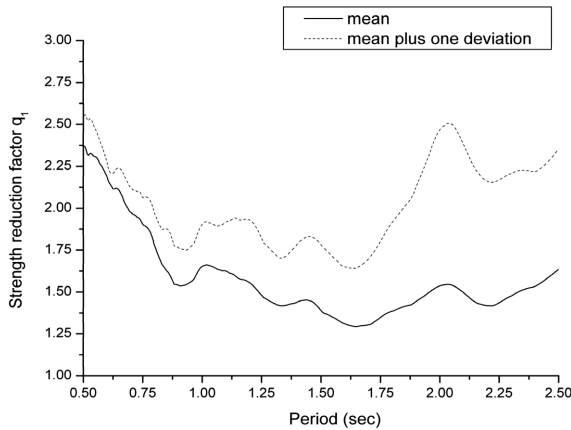
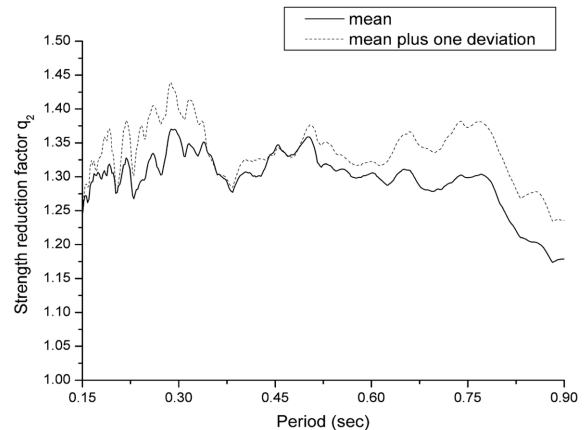
Fig. 10 Mean plus one deviation values of λ versus period for long duration motions

reduction factor that has been calculated on the basis of 5% damping, a value of 5% damping has been subtracted from all equivalent modal damping equations of Table 3. This is necessary as the 5% damping considered is the inherent damping of the structure in the linear region and has nothing to do with the values of equivalent damping given in Table 3 that reflect only nonlinearities (Papagiannopoulos 2008, Papagiannopoulos and Beskos 2010). For modal damping values not provided in Table 3 for the cases of $IDR = 1.5\%$ and 2.5% (pulse motions) and $IDR = 2.0\%$ (long duration motions) which are then taken to be 100%, the corresponding q_k values are obtained from Figs. 3 and 4 for the case of 5%/100%. On the other hand, for modal damping values below 5%, the corresponding q_k values are equal to unity.

Figs. 11-14 illustrate the mean and mean plus one deviation values of the strength reduction factor

Table 4 Mean and mean plus one deviation values of λ as functions of period and damping

Damping	λ (mean values)	λ (mean plus one deviation values)
$\xi = 5\%$	1.0	1.0
$\xi = 8\%$	$1.0/(1.345 - 0.180\sqrt{T} + 0.071 \ln T)$	$1.0/(1 - 0.132\sqrt{T} + 0.152 \ln \xi + 0.055 \ln T)$
$\xi = 10\%$	$1.0/(1.569 - 0.298\sqrt{T} + 0.119 \ln T)$	$1.0/(1.1 - 0.237\sqrt{T} + 0.188 \ln \xi + 0.101 \ln T)$
$\xi = 15\%$	$1.0/(1.962 - 0.515\sqrt{T} + 0.192 \ln T)$	$1.0/(1.1 - 0.493\sqrt{T} + 0.340 \ln \xi + 0.202 \ln T)$
$\xi = 20\%$	$1.0/(2.185 - 0.643\sqrt{T} + 0.218 \ln T)$	$1.0/(1.0 - 0.692\sqrt{T} + 0.463 \ln \xi + 0.266 \ln T)$
$\xi = 25\%$	$1.0/(2.237 - 0.662\sqrt{T} + 0.182 \ln T)$	$1.0/(1.0 - 0.810\sqrt{T} + 0.496 \ln \xi + 0.292 \ln T)$
$\xi = 30\%$	$1.0/(2.020 - 0.424\sqrt{T} - 0.034 \ln T^2)$	$1.0/(1.0 - 0.843\sqrt{T} + 0.487 \ln \xi + 0.275 \ln T)$
$\xi = 40\%$	$1.0/(1.923 - 0.455\sqrt{T} - 0.018 \ln T^2)$	$1.0/(1.0 - 0.851\sqrt{T} + 0.436 \ln \xi + 0.244 \ln T)$
$\xi = 50\%$	$1.0/(1.506 + 0.507\sqrt{T} - 1.198 \ln T)$	$1.0/(1.0 - 0.851\sqrt{T} + 0.378 \ln \xi + 0.258 \ln T)$
$\xi = 60\%$	$1.0/(1.322 + 0.709\sqrt{T} - 1.417 \ln T)$	$1.0/(1.0 - 0.750\sqrt{T} + 0.308 \ln \xi + 0.188 \ln T)$
$\xi = 75\%$	$1.0/(1.128 + 0.811\sqrt{T} - 1.497 \ln T)$	$1.0/(1.0 - 0.650\sqrt{T} + 0.233 \ln \xi + 0.136 \ln T)$
$\xi = 100\%$	$1.0/(0.923 + 0.789\sqrt{T} - 1.399 \ln T)$	$1.0/(1.0 - 0.560\sqrt{T} + 0.154 \ln \xi + 0.116 \ln T)$

Fig. 11 Mean and mean plus one deviation values of the strength reduction factor q_1 (1st mode) versus period for long duration motionsFig. 12 Mean and mean plus one deviation values of the strength reduction factor q_2 (2nd mode) versus period for long duration motions

q_k versus period of the first five modes, i.e. q_1, q_2, q_3, q_4, q_5 , for long duration motions and $IDR = 2.0\%$ and $\theta_p = 3.5\theta_y$. Similarly, Figs.15-17 illustrate the mean and mean plus one deviation values of the strength reduction factor q_k versus period for the first five modes of pulse motions having $M_w > 6.8$ and $IDR = 2.5\%$ and $\theta_p = 6\theta_y$. One can observe that the values of q_k in Figs. 14 and 17 for higher modes (4th and 5th in Fig. 14 and 3rd, 4th and 5th in Fig. 17) are the same as they come from corresponding values of $\xi_k = 100\%$ (overdamped modes). Similar plots for the first five modes of pulse motions having $M_w \leq 6.8$ and $IDR = 2.5\%$ and $\theta_p = 6\theta_y$ as well for all the other cases considering deformation and damage levels of the three categories of seismic motions can be found in Papagiannopoulos (2008).

Finally, design equations for the modal strength reduction factor q_k of the k -th mode are provided in Table 5 as functions of period and according to the type of seismic motion and the deformation

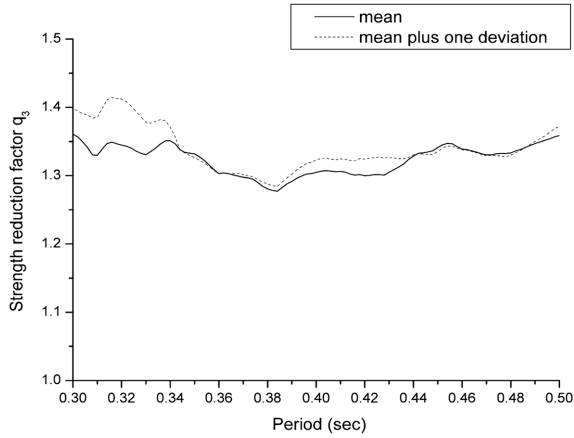


Fig. 13 Mean and mean plus one deviation values of the strength reduction factor q_3 (3rd mode) versus period for long duration motions

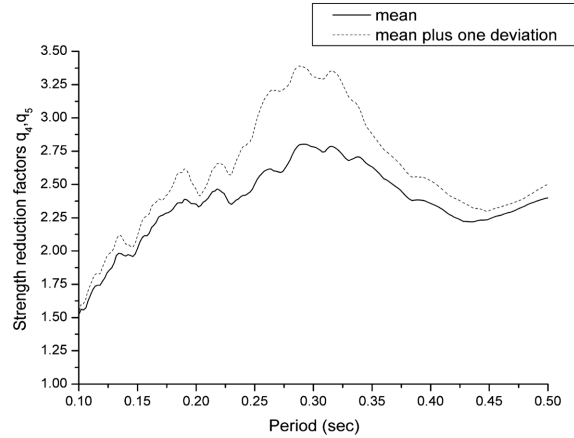


Fig. 14 Mean and mean plus one deviation values of the strength reduction factor q_4, q_5 (4th and 5th modes) versus period for long duration motions

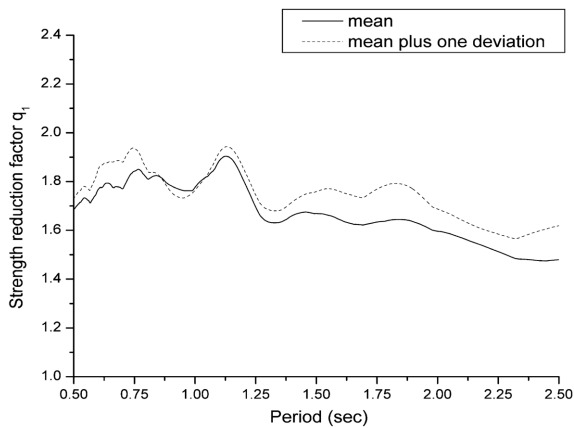


Fig. 15 Mean and mean plus one deviation values of the strength reduction factor q_1 (1st mode) versus period for pulse motions having $M_w > 6.8$

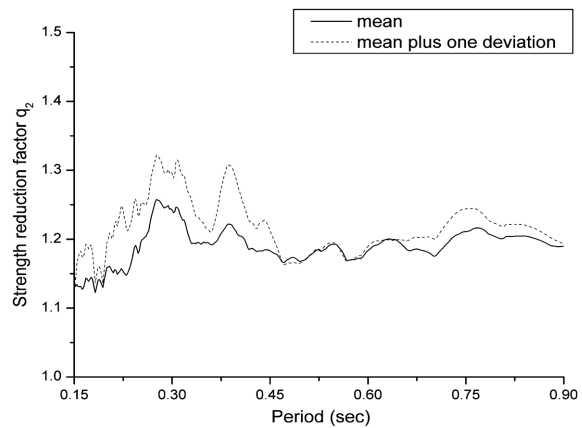


Fig. 16 Mean and mean plus one deviation values of the strength reduction factor q_2 (2nd mode) versus period for pulse motions having $M_w > 6.8$

and damage levels. These equations can be used when damping in the linear region is 5% and provide envelope values of the curves of Figs. 11-17 and those curves that correspond to the case of pulse type motions having $M_w \leq 6.8$ not presented herein due to space limitations. The dashes of Table 5 for $IDR = 2.5\%$ (long duration motions) and $IDR = 2.0\%$ (pulse motions) correspond to no q_k values because the long duration motions could not drive the structures beyond $IDR = 2.0\%$ and the response to pulse motions was not calculated, respectively. Obviously, for the case of $IDR = 0.6\%$ not shown in Table 5, the value of the modal strength reduction factor is equal to unity.

At this point it is important to observe that the values of the modal strength reduction factor are significantly smaller than those found in the literature and the seismic codes. The reason is twofold: a) the modal strength reduction factor is a function of deformation and damage because is calculated by using deformation and damage dependent equivalent modal damping ratios. Due to

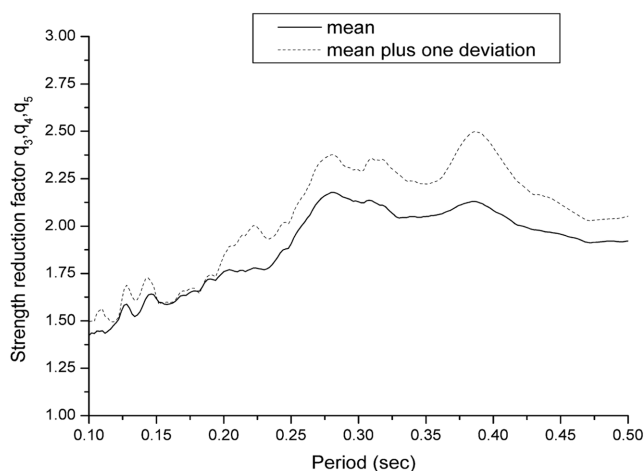


Fig. 17 Mean and mean plus one deviation values of the strength reduction factor q_3 , q_4 , q_5 (3rd, 4th and 5th modes) versus period for pulse motions having $M_w > 6.8$

this deformation dependence of q_k , deformation restrictions imposed on the structure, imply lower values of q_k than the maximum one suggested in seismic codes; b) the modal strength reduction factor is calculated with the aid of the damping reduction factor defined on the basis of absolute acceleration spectra and not pseudo-acceleration spectra (see again Figs. 3-8). However, when the modal strength reduction values q_k are expressed in terms of pseudo-acceleration spectra with the aid of Eq. (8), they become \bar{q}_k and attain higher values close to those in the literature and the seismic codes. It should be also noted that the proposed approach can be extended to other types of structures, e.g. concrete structures, where different values of the modal strength reduction factor would be expected.

5. Numerical examples

In this section some numerical examples are presented in order to illustrate the use of the modal strength reduction factor in seismic design and demonstrate its advantages. In these examples, mean plus one deviation values of response quantities are used just for the sake of illustration as both mean and mean plus one deviation values are equally important.

5.1 One storey and one bay frame

Consider first a steel plane moment resisting frame consisting of one storey and one bay, which can be modelled as a SDOF structure with $\xi = 0\%$, mass $m = 24480$ kgr and $T = 0.6$ sec and determine its design base shear for the case of $IDR = 2.0\%$ and $\theta_p = 3.5\theta_y$. From Table 3 one obtains $\xi = 47\%$. Constructing the 47% damped spectra (mean plus one deviation) for the long duration motions considered here and corresponding to the absolute acceleration and pseudo-acceleration cases, the following values of the design base shear are obtained: $V_{S_a} = 94.85$ kN from the absolute acceleration spectrum and $V_{pS_a} = 63.87$ kN from the pseudo-acceleration spectrum.

The SDOF structure is then subjected to the long duration motions considered here and nonlinear

Table 5 Design equations for the modal strength reduction factor q_k

Seismic motions	Mode	$IDR = 1.5\% \ \& \ \theta_p = \theta_y$	$IDR = 2.0\% \ \& \ \theta_p = 3.5\theta_y$	$IDR = 2.5\% \ \& \ \theta_p = 6\theta_y$
$M_w \leq 6.8$	1	$q = 1.10$ for $0.5 \leq T \leq 2.5$ sec	-	$q = 0.877 \cdot e^{(-T/1.123)} + 1.325$ for $0.50 \leq T \leq 2.50$ sec
	2	$q = 1.00$ for $0.15 \leq T \leq 0.85$ sec	-	$q = 2.50 \cdot (T - 0.10) + 1.50$ for $0.15 \leq T \leq 0.30$ sec & $q = 2.00$ for $0.30 \leq T \leq 0.85$ sec
	3	$q = 1.00$ for $0.11 \leq T \leq 0.48$ sec	-	$q = 2.50 \cdot (T - 0.10) + 1.50$ for $0.11 \leq T \leq 0.30$ sec & $q = 2.00$ for $0.30 \leq T \leq 0.48$ sec
	4	$q = 1.00 \cdot (T - 0.10) + 1.50$ for $0.11 \leq T \leq 0.32$ sec	-	$q = 2.50 \cdot (T - 0.10) + 1.50$ for $0.11 \leq T \leq 0.32$ sec
	5	$q = 1.00 \cdot (T - 0.10) + 1.50$ for $0.10 \leq T \leq 0.24$ sec	-	$q = 2.50 \cdot (T - 0.10) + 1.50$ for $0.10 \leq T \leq 0.24$ sec
$M_w > 6.8$	1	$q = 1.10$ for $0.5 \leq T \leq 2.5$ sec	-	$q = 1.70$ for $0.50 \leq T \leq 1.20$ sec $q = 0.154 \cdot (1.20 - T) + 1.70$ for $1.20 \leq T \leq 2.50$ sec
	2	$q = 1.00$ for $0.15 \leq T \leq 0.85$ sec	-	$q = 1.20$ for $0.15 \leq T \leq 0.85$ sec
	3	$q = 1.00$ for $0.11 \leq T \leq 0.48$ sec	-	$q = 3.33 \cdot (T - 0.10) + 1.40$ for $0.11 \leq T \leq 0.25$ sec & $q = 1.90$ for $0.25 \leq T \leq 0.48$ sec
	4	$q = 1.50 \cdot (T - 0.10) + 1.40$ for $0.11 \leq T \leq 0.32$ sec	-	$q = 3.33 \cdot (T - 0.10) + 1.40$ for $0.11 \leq T \leq 0.25$ sec & $q = 1.90$ for $0.25 \leq T \leq 0.48$ sec
	5	$q = 1.50 \cdot (T - 0.10) + 1.40$ for $0.10 \leq T \leq 0.24$ sec	-	$q = 3.33 \cdot (T - 0.10) + 1.40$ for $0.11 \leq T \leq 0.25$ sec & $q = 1.90$ for $0.25 \leq T \leq 0.48$ sec
Long duration	1	$q = 1.292 + 2 \cdot 10^{-5} e^{3.775T}$ for $0.5 \leq T \leq 2.50$ sec	$q = 2.112 \cdot e^{(-T/5.205)} + 0.001$ for $0.5 \leq T \leq 2.50$ sec	-
	2	$q = 1.00$ for $0.15 \leq T \leq 0.85$ sec	$q = 1.30$ for $0.15 \leq T \leq 0.60$ sec & $q = 0.267 \cdot (0.60 - T) + 1.30$ for $0.60 \leq T \leq 0.85$ sec	-
	3	$q = 1.00$ for $0.11 \leq T \leq 0.48$ sec	$q = 1.32$ for $0.32 \leq T \leq 0.47$ sec	-
	4	$q = 1.00$ for $0.11 \leq T \leq 0.32$ sec	$q = 6.00 \cdot (T - 0.10) + 1.60$ for $0.11 \leq T \leq 0.25$ sec & $q = 2.50$ for $0.25 \leq T \leq 0.48$ sec	-
	5	$q = 1.00$ for $0.10 \leq T \leq 0.24$ sec	$q = 6.00 \cdot (T - 0.10) + 1.60$ for $0.11 \leq T \leq 0.25$ sec & $q = 2.50$ for $0.25 \leq T \leq 0.48$ sec	-

dynamic analyses provide a yielding base shear of $V_y = 89.73$ kN. Thus, the base shear of the SDOF structure found by using the absolute acceleration spectrum is very close (error = 5.7%) to the 'exact' value of the nonlinear dynamic analysis, while the one found by using the pseudo-acceleration spectrum is far apart from it (error = 28.8%). Moreover, the strength reduction factor associated with the 'exact' absolute acceleration spectrum is found with the aid of Fig. 3 to be $q_1 = 2.19$, while the one associated with the pseudo-acceleration spectrum is found with the aid of Fig. 5 to be $\bar{q}_1 = 3.24$, i.e. in error equal to 47.95% as compared to the value $q_1 = 2.19$. Finally, one can observe that multiplication of the pseudo-acceleration spectral value of 63.87 kN for the design base shear by the corresponding mean value of the ratio n of Fig. 7 gives 94.85 kN, i.e. exactly the value of the design base shear obtained by using the absolute acceleration spectrum.

5.2 Twelve storey and four bay frame : case 1

Consider now a steel plane moment resisting framed structure consisting of twelve stories and four bays. Each bay of the steel frame has 4.0 m span and each storey 3.0 m height. The dead plus live load on beams is equal to 27.5 kN/m and the expected ground motion is defined by using the mean plus one deviation 5% damped absolute acceleration spectrum for the long duration motions considered herein. HEB profiles are used for columns and IPE for beams. Target values for IDR and θ_p are equal to 2.0% and $3.5\theta_y$, respectively. The design starts with the following sections: 360/360/360/360/360-400 (1-5) & 340/340/340/340/340-360 (6-9) & 300/300/300/300/300-300 (10-12). In the above, expressions of the form, e.g. 360/360/360/360/360-400 (1-5) mean that every storey from 1 to 5 has columns with HEB360 sections and beams with IPE400 sections at every bay of that storey. For this section selection one can find the first five natural periods of the frame to be $T_1 = 1.83$, $T_2 = 0.65$, $T_3 = 0.38$, $T_4 = 0.25$, $T_5 = 0.19$ secs. The modal strength reduction factor values q_k are obtained from Figs. 11-14 and read $q_1 = 1.96$, $q_2 = 1.36$, $q_3 = 1.29$, $q_4 = 2.96$, $q_5 = 2.59$. Thus, with the aid of SAP 2000 (2005) one can easily determine through modal synthesis/spectrum analysis the design base shear of the frame as equal to 132.3 kN.

The above modal values of the strength reduction factor cannot be used directly in SAP 2000 (2005) because only one value of the strength reduction factor can be considered there. For this reason, an artificial design spectrum is inserted in SAP 2000 (2005) with ordinates for the periods needed evaluated as follows: the ordinates of the aforementioned mean plus one deviation 5% damped absolute acceleration spectrum of the motions considered here, which are defined for the periods needed, are divided by the corresponding values of the modal reduction factor. Thus, by performing spectrum analysis in SAP 2000 (2005) one can prove with the aid of EC3 (1992) that the original section selection was the right one.

Non – linear dynamic analyses are then executed using the accelerograms of the long duration motions considered previously. From these analyses one can obtain a) the yielding base shear (the shear at first plastic hinge formation), considered to be the 'exact' solution, equal to 127 kN, which is very close to the design base shear of 132.3 kN and b) the mean values of $IDR = 1.86\%$ and $\theta_p = 3.13\theta_y$, which are very close to the target ones. It should be stressed that the aforementioned spectrum analysis cannot give an estimate of non-linear deformation, as usually done by applying the equal displacement approximation, because the strength reduction factor does not have a common value for all modes. Nevertheless, this is not a matter of concern as the modal strength reduction factor is given as function of deformation and thus, as proven by non – linear dynamic analysis, the desired deformation limits are automatically satisfied.

5.3 Twelve storey and four bay frame : case 2

In the previous example, the proposed method employed an absolute acceleration spectrum constructed on the basis of the data of the present work. In the example that follows, the proposed method makes use of the elastic design spectrum of EC8 (2004) (PGA = 0.24 g, 5% damping and soil class B) that corresponds to pseudo-acceleration, which as mentioned previously, lacks accuracy for high levels of damping in comparison to the absolute acceleration spectrum. Thus, if one wants to use the pseudo-acceleration spectrum of EC8 (2004) in conjunction with the proposed modal strength reduction factor, use should be made of Eq. (8) in order to convert it into the corresponding absolute acceleration spectrum. This is exactly what is done in the present example where use is first made of the q_k values of Figs. 11-14 rather than Table 5 for increased accuracy. Use of Table 5 is done subsequently.

On the basis of the section selection of the previous example and the corresponding first five natural periods one can obtain from Table 3 the first five ξ values for $IDR = 2.0\%$ and $\theta_p = 3.5\theta_y$. For these ξ values, Table 4 provides the mean plus one deviation values of λ to be used in Eq. (8) for the determination of $S_d(T, \xi)$ and from there of the q_k through Eq. (4). The resulting values of q_k are: $q_1 = 1.77$, $q_2 = 1.32$, $q_3 = 1.29$, $q_4 = 1.27$, $q_5 = 1.27$. By performing spectrum analysis in SAP 2000 (2005) as before and by using the above values of the modal strength reduction factor, the design base shear is found equal to 134 kN. Non – linear dynamic analyses are then executed using the long duration accelerograms of this work, compatible to the absolute acceleration converted EC8 (2004) design spectrum and provide the yielding base shear of the frame equal to 126 kN. The above design value of the proposed method equal to 134 kN is very close (error 6.3%) to the ‘exact’ value of 126 kN.

The same steel frame is now designed by the proposed method by using the 5% damped elastic pseudo-acceleration spectrum of EC8 (2004) with PGA = 0.24 g, soil class B and the damping reduction factor expression $\sqrt{10/(5 + \xi)} \geq 0.55$. Use of Table 1 for $IDR = 2.0\%$ and $\theta_p = 3.5\theta_y$, as before, provides the first five ξ values to be used in Eq. (6) with $\bar{B}_a = \sqrt{10/(5 + \xi)} \geq 0.55$ to obtain the \bar{q}_k values as $\bar{q}_1 = 1.82$, $\bar{q}_2 = 1.27$, $\bar{q}_3 = 1.22$, $\bar{q}_4 = 1.82$ and $\bar{q}_5 = 1.82$. By performing spectrum analysis in SAP 2000 (2005) in conjunction with the aforementioned values of \bar{q}_k , the design base shear is found equal to 130 kN. Non – linear dynamic analyses are then executed using the long duration accelerograms of this work, compatible to the aforementioned EC8 (2004) pseudo-acceleration design spectrum, and the yielding base shear of the frame is found to be equal to 120 kN. The previously found design value of 130 kN is close (error 8.33%) to this ‘exact’ value of 120 kN. However, the error between 130 kN in this case and 134 kN in the previous case is considered to be small because the \bar{q}_k values are very close to the true values q_k , i.e. $q_1 = 1.77$, $q_2 = 1.32$, $q_3 = 1.29$, $q_4 = 1.27$, $q_5 = 1.27$ and because according to the code $\bar{B}_a \geq 0.55$. The influence of the 4th and 5th modes is also small and, thus, the difference between \bar{q}_4 and q_4 and \bar{q}_5 and q_5 does not create any problem. Nevertheless, a larger difference in the value of the design base shear is expected between the cases using \bar{q}_k instead of q_k when there is greater higher mode participation.

The twelve storey and four bay steel frame is finally designed by employing the conventional method of EC8 (2004) that makes use of a single value of the strength reduction (behavior) factor in conjunction with the deformation restriction of $IDR = 2.0\%$ and compared with the proposed method associated with the use of Table 5 for the design values of q_k . For the frame type considered, one has that $q = 6$. The design starts with the following initial section selection: 240/

260/260/260/240-240 (1-5) & 240/260/260/260/240-240 (6-9) & 220/240/240/240/220-240 (10-12). For this section selection, one finds $IDR = 2.89\%$. Using the aforementioned 5% damped elastic pseudo-acceleration spectrum of EC8 (2004) with $q = 6$ and enforcing the $IDR = 2.0\%$ restriction through the equal displacement rule, the following sections are found after some iterations: 300/300/300/300-270 (1-5) & 280/280/280/280/280-270 (6-9) & 260/260/260/260/260-240 (10-12). Non – linear dynamic analyses executed in conjunction with the long duration accelerograms of this work, compatible to the aforementioned EC8 (2004) design spectrum, produce an IDR value equal to 1.74% indicating that this value is in an error of about 9% due to the use of the approximate equal displacement rule. It is clear that heavier sections had to be selected in order to satisfy the $IDR = 2.0\%$ limit.

Thus, no matter how large is the initially chosen value of q from EC8 (2004), if one has to satisfy certain deformation requirements, he will be finally led to heavier sections indicating that a smaller value of q should have been chosen. If such a value is assumed to be $q = 2$, which is close to the q_k values of the proposed method, the sections found are 400/400/400/400/400-400 (1-5) & 360/360/360/360-360 (6-9) & 320/320/320/320/320-360 (10-12) with a maximum $IDR = 1.59\%$. This design is now compared to the design obtained by the proposed method in conjunction with the use of the design values of q_k given in Table 5. The starting sections are assumed to be the same with the final ones of the previous design, i.e. 400/400/400/400/400-400 (1-5) & 360/360/360/360/360-360 (6-9) & 320/320/320/320/320-360 (10-12). The pseudo-acceleration spectrum of EC8 (2004) is now converted to its absolute counterpart with the aid of the mean plus one deviation values of λ from Table 4 and the use of Eq. (8). This absolute acceleration spectrum is used in conjunction with the design values q_k ($q_1 = 1.49$, $q_2 = 1.29$, $q_3 = 1.32$, $q_4 = 2.50$, $q_5 = 2.12$) obtained from Table 5 to arrive at the final sections 360/360/360/360/360-400 (1-5) & 340/340/340/340/340-360 (6-9) & 300/300/300/300-300 (10-12) which represent a lighter section selection. Furthermore, non – linear dynamic analyses executed in conjunction with the accelerograms of the long duration motions considered previously yield an $IDR = 1.86\%$, which is much closer to the target value of $IDR = 2.0\%$ than the value of $IDR = 1.59\%$ of the previous design.

On the basis of the above results, it is obvious that the proposed method based on modal strength reduction factors in comparison to the conventional method of employing a common value of the behavior factor leads to results of better accuracy. In general, from these design examples and others not shown herein due to space limitations, it is concluded that the proposed method offers significant advantages over the conventional method regarding the desired seismic performance level because a) recognizes the different modal contributions to the design base shear, b) uses deformation and damage dependent values of the reduction factor, c) employs a conversion of pseudo-acceleration into absolute acceleration and d) avoids the equal displacement approximation.

6. Conclusions

On the basis of the preceding developments, the following conclusions can be stated:

- 1) A seismic design method for plane steel moment resisting frames has been developed. The method employs the modal strength reduction factor, spectrum analysis and modal synthesis. The modal strength reduction factor is obtained by combining equivalent modal damping ratios and damping reduction factors used to construct absolute or pseudo-acceleration spectra with high damping values.

- 2) Curves relating modal strength reduction factor with period, deformation and damage have been constructed and corresponding design equations have been developed. These curves or equations can be used in conjunction with design spectrum and modal synthesis tools to calculate the design base shear of the structure.
- 3) The proposed approach was applied to the seismic design of steel moment resisting framed structures and was validated using non – linear inelastic dynamic analyses. Unlike the usual code – based approach which considers a single strength reduction factor value for all modes, the proposed approach employing different modal strength reduction factors leads to more accurate results.
- 4) In comparison to the method which employs modal damping ratios (Papagiannopoulos 2008, Papagiannopoulos and Beskos 2010), the proposed method appears to be a better choice since it can be used directly with the existing 5% damped pseudo-acceleration spectra of EC8 (2004).

References

- Borzi, B. and Elnashai, A.S. (2000), “Refined force reduction factors for seismic design”, *Eng. Struct.*, **22**, 1244-1260.
- Chai, Y.H., Fajfar, P. and Romstad, K.M. (1998), “Formulation of duration-dependent inelastic seismic design spectrum”, *J. Struct. Eng. - ASCE*, **124**(8), 913-921.
- Chakraborti, A. and Gupta, V.K. (2005), “Scaling of strength reduction factors for degrading elasto-plastic oscillators”, *Earthq. Eng. Struct. Dyn.*, **34**, 189-206.
- Cuesta, I., Aschheim, M.A. and Fajfar, P. (2003), “Simplified R-factor relationships for strong ground motions”, *Earthq. Spectra*, **19**(1), 25-45.
- EC3 (1992), *Eurocode 3, Design of steel structures, Part 1.1: General rules for buildings*, European Prestandard ENV 1993-1-1/1992, European Committee for Standardization (CEN), Brussels.
- EC8 (2004), *Eurocode 8, Design of structures for earthquake resistance, Part 1: General rules, seismic actions and rules for buildings*, European Standard EN 1998-1, Stage 51 Draft, European Committee for Standardization (CEN), Brussels.
- Englekirk, R.E. (2008), “A call for change in seismic design procedures”, *Struct. Des. Tall Spec. Bldgs*, **17**, 1005-1013.
- Jalali, R.S. and Trifunac, M.D. (2008), “A note on strength-reduction factors for design of structures near earthquake faults”, *Soil Dyn. Earthq. Eng.*, **27**, 212-222.
- Karavasilis, T.L., Bazeos, N. and Beskos, D.E. (2007), “Behavior factor for performance-based seismic design of plane steel moment resisting frames”, *J. Earthq. Eng.*, **11**, 531-559.
- Kunnath, S.K. and Chai, Y.H. (2004), “Cumulative damage-based inelastic cyclic demand spectrum”, *Earthq. Eng. Struct. Dyn.*, **33**, 499-520.
- Lin, Y.Y. and Chang, K.C. (2003), “Study on damping reduction factor for buildings under earthquake ground motions”, *J. Struct. Eng. - ASCE*, **129**(2), 206-214.
- Lu, Y. and Wei, J. (2008), “Damage-based inelastic response spectra for seismic design incorporating performance considerations”, *Soil Dyn. Earthq. Eng.*, **28**, 536-549.
- Mavroeidis, G.P., Dong, G. and Papageorgiou, A.S. (2004), “Near-fault ground motions, and the response of elastic and inelastic single-degree-of-freedom (SDOF) systems”, *Earthq. Eng. Struct. Dyn.*, **33**, 1023-1049.
- Mazzolani, F.M. and Piluso, V. (1996), *Theory and design of seismic resistant steel frames*, E & FN Spon, London.
- Miranda, E. and Bertero, V.V. (1994), “Evaluation of strength reduction factors for earthquake-resistant design”, *Earthq. Spectra*, **10**(2), 357-379.
- Mwafy, A.M. and Elnashai, A.S. (2002), “Calibration of force reduction factors of rc buildings”, *J. Earthq. Eng.*, **6**(2), 239-273.

- Nassar, A.A. and Krawinkler, H. (1991), *Seismic demands of SDOF and MDOF structures*, John A. Blume Earthquake Engineering Centre Report No.95, Department of Civil and Environmental Engineering, Stanford University.
- Ordaz, M. and Pérez-Rocha, L.E. (1998), "Estimation of strength-reduction factors for elastoplastic systems: a new approach", *Earthq. Eng. Struct. Dyn.*, **24**, 889-901.
- Papagiannopoulos, G.A. (2008), *Seismic design of steel structures using equivalent modal damping ratios or modal strength reduction factors*, Ph.D. Thesis (in Greek), Department of Civil Engineering, University of Patras, Greece, e-link address: <http://nemertes.lis.upatras.gr/dspace/handle/123456789/2113>.
- Papagiannopoulos, G.A. and Beskos, D.E. (2010), "Towards a seismic design method for plane steel frames by using equivalent modal damping ratios", *Soil Dyn. Earth. Eng.*, **30**, 1106-1118.
- Prakash, V., Powell, G.H. and Campbell, S. (1993), *DRAIN 2DX - Base program description and user guide*, Version 1.10., Report No.UCB/SEMM-93/17, University of California at Berkeley.
- SAP2000 (2005), *Static and dynamic analysis finite element analysis of structures*, Version 9.1.4., Computers and Structures Inc., Berkeley, California.
- Seneviratna, G.D.P.K. and Krawinkler, H. (1997), *Evaluation of seismic MDOF effects for seismic design*, John A. Blume Earthquake Engineering Centre Report No.120, Department of Civil and Environmental Engineering, Stanford University.
- Sullivan, T.J., Priestley, M.J.N. and Calvi, G.M. (2008), "Estimating the higher-mode response of ductile structures", *J. Earthq. Eng.*, **12**, 456-472.
- Takewaki, I. (1997), "Design-oriented ductility bound of a plane frame under seismic loading", *J. Vib. Control*, **3**, 411-434.
- Veletsos, A.S. and Vann, W.P. (1971), "Response of ground-excited elastoplastic systems", *J. Struct. Division - ASCE*, **97**, (ST4), 1257-1281.
- Vidic, T., Fajfar, P. and Fischinger, M. (1994), "Consistent inelastic design spectra: strength and displacement", *Earthq. Eng. Struct. Dyn.*, **23**, 507-521.
- Weitzmann, R., Ohsaki, M. and Nakashima, M. (2006), "Simplified methods for design of base-isolated structures in the long-period high-damping range", *Earthq. Eng. Struct. Dyn.*, **35**, 497-515.